Available online at www.sciencedirect.com
ScienceDirect
Trans. Nonferrous Met. Soc. China 22(2012) s395−s401
Transactions of Nonferrous Metals Society of China
www.tnmsc.cn

Influence of interfacial adhesion strength on formability of AA5052/polyethylene/AA5052 sandwich sheet

LIU Jian-guang[1, 2], LIU Wei[1, 2], WANG Jing-xuan[2]

1. National Key Laboratory for Precision Hot Processing of Metals, Harbin Institute of Technology, Harbin 150001, China;
2. School of Materials Science and Engineering, Harbin Institute of Technology, Harbin 150001, China

Received 28 August 2012; accepted 25 October 2012

Abstract: The effects of interfacial adhesion strength between skin sheet and core polymer on the formability of AA5052/polyethylene/AA5052 sandwich sheets was investigated. A numerical simulation model considering the interface conditions between skin sheet and core materials was developed for simulating the forming process of sandwich sheet. Comparisons between the experimental results and calculations verify the proposed model. Then, the rigid punch tests and the NAKAZIMA forming tests were carried out for sandwich sheets with three kinds of interface conditions (separation, adhesion and stick). The influences of interfacial adhesion strength on the damage behavior of skin sheet and the forming limit diagrams (FLD) of sandwich sheets were investigated. The results show that the interface stress can suppress the increasing of void volume fraction and then postpone the fracture of skin sheet. The FLD of sandwich sheet with stick interfacial condition is higher than those of sandwich sheets with adhesion and separation interfacial conditions. It can be concluded that the FLD of sandwich sheet shifts to higher value with the increasing of interfacial adhesion strength.

Key words: sandwich sheets; formability; interfacial adhesion strength; aluminum; polyethylene; numerical method, damage model

1 Introduction

As a potential light-weight material, metal-plastic sandwich sheets have generated a considerable interest for structural parts to reduce the structure weight [1]. Typically a metal−plastic sandwich sheet consists of two layers of metallic sheet as skin and a polymeric material as core. Three layers are glued together. The skin metallic materials can be steel or aluminium alloy and the core polymeric material is polypropylene or polyethylene generally. Compared with monolithic metallic sheet, metal−plastic sandwich sheet offers a lower density, higher specific flexural stiffness, better dent resistance and better sound and vibration damping characteristics [2, 3]. Due to these advantages, metal−plastic sandwich sheets are gaining increasing applications in aeronautical, marine, automotive industries and civil engineering. Taking automotive industry as example, steel−plastic sandwich sheet, have been used to manufacture some automotive components which are formed by the single steel sheets in order to reduce the weight of whole car, such as dash panel and wheel house inner [4]. Compared with steel−plastic sandwich sheet, aluminium−plastic sandwich sheets provide a lower mass per square meter and higher specific flexural stiffness [5]. Many kinds of aluminium−plastic sandwich sheets have been developed with different aluminium alloys as skin sheet and different plastics as core layer, such as AA5182/polypropylene/AA5182 sandwich sheet [6], AA5005/polypropylene/AA5005 sandwich sheet [7], and AA3105/polypropylene/AA3105 sandwich sheet [8]. Among these sandwich sheets, AA5182/polypropylene/AA5182 sandwich sheet have been developed for potential application of these materials for automotive body panels in future high performance automobiles with significant mass reduction [6].

However, the behaviour of the sandwich sheet is quite different from those of homogenous metallic sheets during forming processes. The interface stress between skin sheet and core layer has a large influence on the

Foundation item: Project (HIT.NSRIF.2009033) supported by the Fundamental Research Funds for the Central Universities, China
Corresponding author: LIU Jian-guang; Tel/Fax: +86-451- 86413365-19; E-mail: liujg@hit.edu.cn
DOI: 10.1016/S1003-6326(12)61737-3

deformation behaviour of sandwich sheet [9]. Furthermore, the sliding and shearing occur between skin layers and hence affect the formability of the sandwich sheet. But none of research has been done to investigate the effects of interface condition between skin sheet and core materials on the formabilities of sandwich sheets.

In the present work, a numerical simulation model considering the interface conditions between skin sheet and core materials was developed for simulating the forming process of sandwich sheet. Experiments and numerical simulations of rigid punch tests and the NAKAZIMA forming tests were conducted. Comparisons between the experimental results and calculations were made to verify the proposed model. Then, the rigid punch tests and the Nakazima forming tests were simulated for sandwich sheets with three kinds of interfacial conditions (separation, adhesion and stick). The influences of interfacial adhesion strength on the damage behavior of skin sheet and the forming limit diagrams (FLD) of sandwich sheets were investigated.

2 Determination of sheet metal forming limit diagrams

2.1 GTN continuum damage model

The Gurson-Tvergaard-Needleman (GTN) continuum damage model was used to describe the skin sheet of sandwich sheet. The GTN damage model was extensively used to analyze the sheet metal forming, such as predicting formability, analyzing the void evolution, and so on [10−13]. Different from the constitutive laws that follow the classic J_2 criterion and are independent of hydrostatic pressure, the yield function of GTN continuum damage material model is a pressure-sensitive yield function and can be expressed as [12]

$$\Phi=\left(\frac{q}{\sigma_y}\right)^2+2q_1f^*\cosh\left(-q_2\frac{3p}{2\sigma_y}\right)-\left(1+q_3f^{*2}\right)=0 \tag{1}$$

where q denotes the macroscopic von Mises equivalent stress, $q=\sqrt{3S_{ij}S_{ij}/2}$; S_{ij} is the deviatoric part of the Cauchy stress tensor σ_{ij}, $S_{ij}=\sigma_{ij}-\sigma_{kk}\delta_{ij}/3$, δ_{ij} represents the KRONECKER delta; σ_y is the equivalent flow stress which represents the actual microscopic stress state in the matrix material; p is the hydrostatic stress; q_1, q_2 and q_3 are introduced by Tvergaard to make the predictions of Gurson's equations agree with numerical studies of materials containing periodically distributed circular cylindrical voids. When q_1=q_2=q_3=1, the GTN model recovered to Gurson model. f^* is the damage parameter introduced by Tvergaard and Needleman, which denotes the total effective void volume fraction [13,14]. It accounts for the gradual loss of stress carrying capability of the material due to void coalescence. f^*=0 implies that the material is fully dense, and the Gurson yield condition reduces to the von Mises yield condition. f^*=1 implies that the material is completely voided and has no stress carrying capacity. This function is defined in terms of the void volume fraction:

$$f^*=\begin{cases}f,\text{if } f\le f_c\\ f_c+\dfrac{\bar{f}_F-f_c}{f_F-f_c}(f-f_c),\text{if } f_c<f<f_F\\ \bar{f}_F,\text{if } f\ge f_F\end{cases} \tag{2}$$

in which

$$\bar{f}_F=\frac{q_1+\sqrt{q_1^2-q_3}}{q_3} \tag{3}$$

where f is the void volume fraction, f_c is a critical value of the void volume fraction, f_F is the value of void volume fraction at which there is a complete loss of stress carrying capacity in the material. The user specified parameters f_c and f_F model the material failure when f_c<f<f_F, due to mechanisms such as micro fracture and void coalescence. When f≥f_F, total failure at the material point occurs.

The increased rate of total void volume fraction $\dot{f}$ is partly due to the growth of existing voids $\dot{f}_g$ and partly due to the nucleation of new voids $\dot{f}_n$ as

$$\dot{f}=\dot{f}_g+\dot{f}_n \tag{4}$$

The growth rate of voids $\dot{f}_g$ is proportional to the hydrostatic component of the plastic strain rate $\dot{\varepsilon}_{kk}^p$, as follows:

$$\dot{f}_g=(1-f)\dot{\varepsilon}_{kk}^p \tag{5}$$

The nucleation rate of new voids can be expressed by a plastic strain-controlled nucleation rule through assuming that voids nucleate at second phase particles and there exists a normal distribution of nucleation strain for the total population of particles:

$$\dot{f}_n=\frac{f_N}{s_N\sqrt{2\pi}}\exp\left[-\frac{1}{2}\left(\frac{\bar{\varepsilon}^p-\varepsilon_N}{s_N}\right)^2\right]\dot{\bar{\varepsilon}}^p \tag{6}$$

where f_N represents the volume fraction of void-nucleating particles, ε_N and S_N are the average and standard deviation of the strains at which particles nucleate voids.

2.2 Interfacial adhesion model

The cohesive zone modeling (CZM) was used to simulate the interfacial adhesion condition between skin aluminum-alloy sheet and core polymer. CZM can be used to model the delamination at interfaces directly in terms of traction versus separation using a traction-

separation law. CZM assumes a linear elastic traction-separation law prior to damage and assumes that failure of the cohesive bond is characterized by progressive degradation of the cohesive stiffness, which is driven by a damage process.

Damage is assumed to initiate when a quadratic interaction function involving the contact stress ratios (as defined in the expression below) reaches a value of one. This criterion can be represented as

$$\left\{\frac{\langle t_n \rangle}{t_n^0}\right\}^2 + \left\{\frac{t_s}{t_s^0}\right\}^2 + \left\{\frac{t_t}{t_t^0}\right\}^2 = 1 \quad (7)$$

where t_n, t_s and t_t refer to the stress in the normal, the first, and the second shear directions, respectively. t_n^0, t_s^0 and t_t^0 represent the peak values of the contact stress when the separation is either purely normal to the interface or purely in the first or the second shear direction, respectively.

The dependence of the fracture energy on the mode mix can be defined based on a power law fracture criterion. The power law criterion state that failure under mixed-mode conditions is governed by a power law interaction of the energies required to cause failure in the individual (normal and two shear) modes. It is given by

$$\left\{\frac{G_n}{G_n^C}\right\} + \left\{\frac{G_s}{G_s^C}\right\} + \left\{\frac{G_t}{G_t^C}\right\} = 1 \quad (8)$$

where G_n, G_s and G_t refer to the work done by the traction and its conjugate separation in the normal, the first, and the second shear directions respectively. G_n^C, G_s^C and G_t^C refer to the critical energies required to cause failure in the normal, the first and the second shear directions, respectively.

2.3 Nakazima forming test

For investigating the formability and determining the forming limit diagram (FLD) of sandwich sheets, the rigid punch tests and the Nakazima forming tests according to the International Deep Drawing Research Group (IDDRG) were carried out on a universal materials testing machine at room temperature [15]. The used sheet metal samples had the same diameter but four different widths, varying from 20 mm to 80 mm (Fig. 1(a)). The samples were pressed until fracture occurs by a hemispherical punch with a diameter of 90 mm and a punch speed of 3 mm/s. The strain paths of the arc-shaped specimens are located in the negative minor strain region, which covers the region from the simple tension region to the plane strain region; and the strain paths of the circle specimens cover the plane strain region to the balanced biaxial stretch region. Two lubrication conditions were applied to the punch-stretch tests. The friction coefficient decreases in the order of dry, polytetrafluoroethene film. Each arc-shaped specimen has one specific strain path on the FLD with the same lubricant (P), and the circle specimens were deformed with different lubricants (dry and P) to obtain the biaxial stretch. The test specimens are shown in Fig. 1(b). The circle grids (each with a diameter of

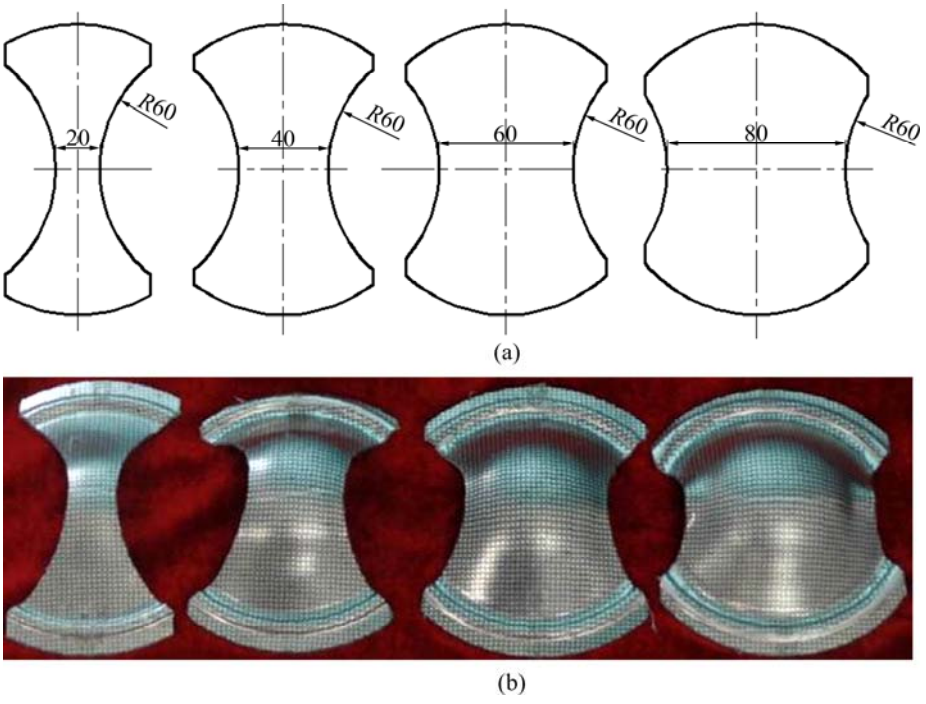

Fig. 1 Main dimensions of test samples (a) and experimental specimens (b) (Unit: mm)

2.0 mm) were printed on the surface of test samples to measure the strain of specimens after testing. After tests, the strain of specimens was analyzed by using an optical measuring system. An ASAME software program simultaneously computed the strains close to the cracking area. By means of measured critical maximum and middle strains at fracture in a limiting curve was plotted for every different specimen dimensions.

3 Finite element analysis

3.1 Finite element model

The commercial FEA software package ABAQUS/Explicit was used to conduct the numerical investigations. A factor of 1000 was set for mass scaling to reduce computation times. Considering the symmetric of geometry structure, one fourth of the workpiece was modeled. The nodes of the sheet falling on the symmetrical axes were constrained in the matching direction. A three-layer sandwich sheet with face sheets of aluminum alloy 5052-O and central sheet of polyethylene was construed. The interface between skin sheet and core polyethylene was set to different conditions. In the numerical simulations, frictional effects were taken into account by means of the Coulomb model. In order to simulate utilization of lubricants, the friction coefficient between punch and sandwich sheet, sandwich sheet and die were set equal to 0.1 and 0.06, respectively. Figure 2 shows the finite element model of formability tests.

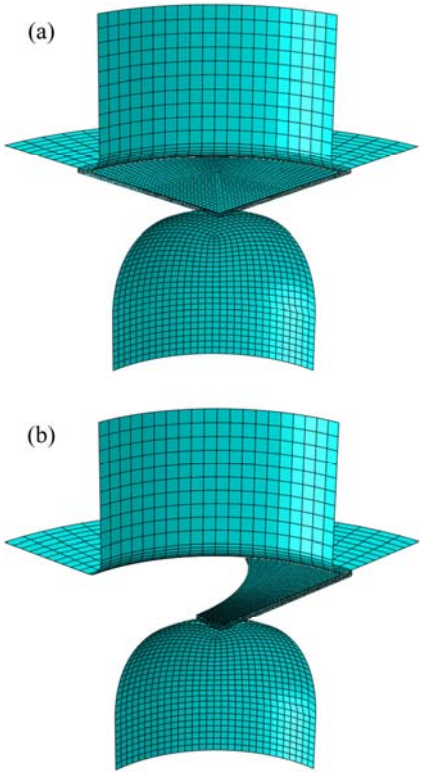

Fig. 2 Finite element models of dome tests (a) and Nakazima tests (b)

3.2 Sandwich sheets

An AA5052/polyethylene/AA5052 sandwich sheet was used in this work. The thickness of AA5052-O aluminium alloy sheet and polyethylene were 0.5 mm and 1.0 mm respectively. The AA5052/polyethylene/AA5052 sandwich sheets were fabricated by using hot-pressing method. The engineering strain-nominal stress curves of AA5052-O skin sheet and polyethylene core materials are shown in Fig. 3, which were obtained by conducting the tensile tests.

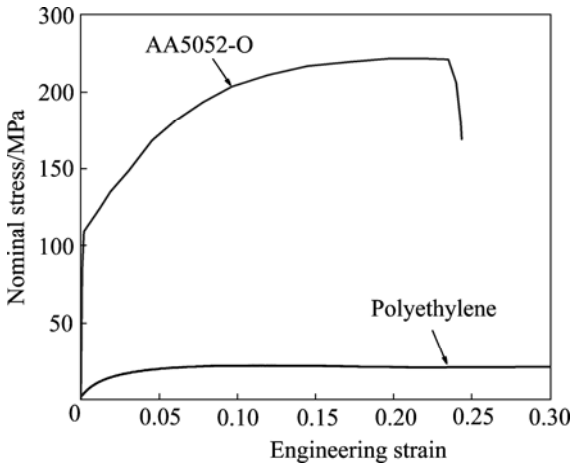

Fig. 3 Stress—strain curves of AA5052-O skin sheet and polyethylene core

The GTN damage constants of AA5052-O are listed in Table 1. These constants were identified by using a hybrid numerical−experimental method. The detailed procedure for determining these constants can be found in Ref. [16].

Table 1 GTN damage constants of AA5052-O [16]

q_1	q_2	q_3	f_N	f_c	f_F	ε_N	S_N	f_0
1.5	1	2.25	0.025	0.027	0.043	0.1	0.1	0.003

3.3 Interfacial conditions between skin sheet and core polymer

The cohesive zone model (CZM) was used to simulate the interfacial adhesion condition between the skin aluminium alloy sheet and core polymer. In order to investigate the influence of interfacial adhesion strength on the formability of sandwich sheet, three interfacial conditions (separation, adhesion and stick) were considered. Table 2 shows the FEA realization of these three interfacial conditions. For the condition of adhesion, the CZM model was used. Table 3 shows the CZM

parameters used in the numerical simulations. The detailed procedure for determining these parameters can be found in Ref. [16].

Table 2 Three interfacial conditions and FEA realization

Case	Interfacial condition	FEA realization
1	Separation	Column friction
2	Adhesion	CZM
3	Stick	Tie

Table 3 CZM parameters [16]

t_n^0 / MPa	t_s^0 / MPa	t_t^0 / MPa	G_n^C / (J·m^{-2})	G_s^C / (J·m^{-2})	G_t^C / (J·m^{-2})
5.3	8.8	8.8	200	295	295

4 Results and discussion

4.1 Validation of numerical simulation model

The punch loads obtained from the simulations for test specimens with different widths are shown in Fig. 4. The fluctuation in the load—stroke curve observed in the simulation was due to the oscillation of nodes in contact with the punch. The punch load increases with increasing the width of test specimens. The predicted punch loads have good agreement with the experimental ones. Then, the proposed numerical simulation model for sandwich sheet was validated.

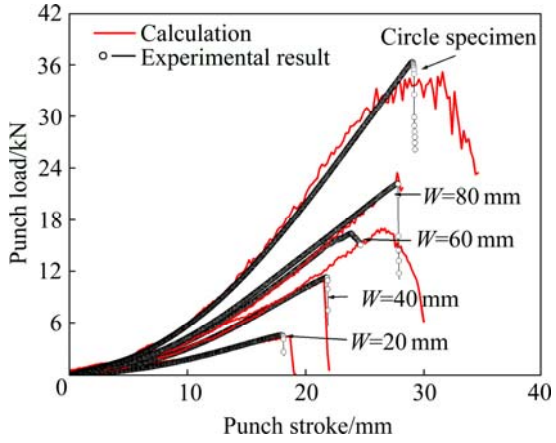

Fig. 4 Punch load obtained from FE simulations and experiments

4.2 Void volume fraction

The void volume fraction (VVF) of skin sheet for three cases was analyzed to investigate the influence of interfacial adhesion strength on the deformation behaviour of sandwich sheet. Figure 5 shows the comparisons of VVF distributions of skin sheet for three sandwich sheets at the dome height of 25 mm. For outer skin sheet, the maximum VVF occurs at the dome centre of specimen for Case 1. But for the other two cases, the maximum VVF occurs at the "mountainside" of the specimen. For inner skin sheet, the maximum VVF occurs at the "mountainside" of the specimen for all three cases. But the maximum VVF value of inner skin sheet for Case 1 is far higher than those for the other two cases. Furthermore, the maximum VVF of skin sheet for Case 2 is a little higher than that of skin sheet for Case 3. It can be explained by that the interface stress between skin sheet and core polymer suppresses the increase of VVF. For Case 1, because of the separation condition between skin sheet and core polymer, the friction between punch and skin sheet has great effect on the deformation behaviour of inner skin sheet but none effect on that of outer skin sheet. So, these two skin sheets show distinct deformation behaviour.

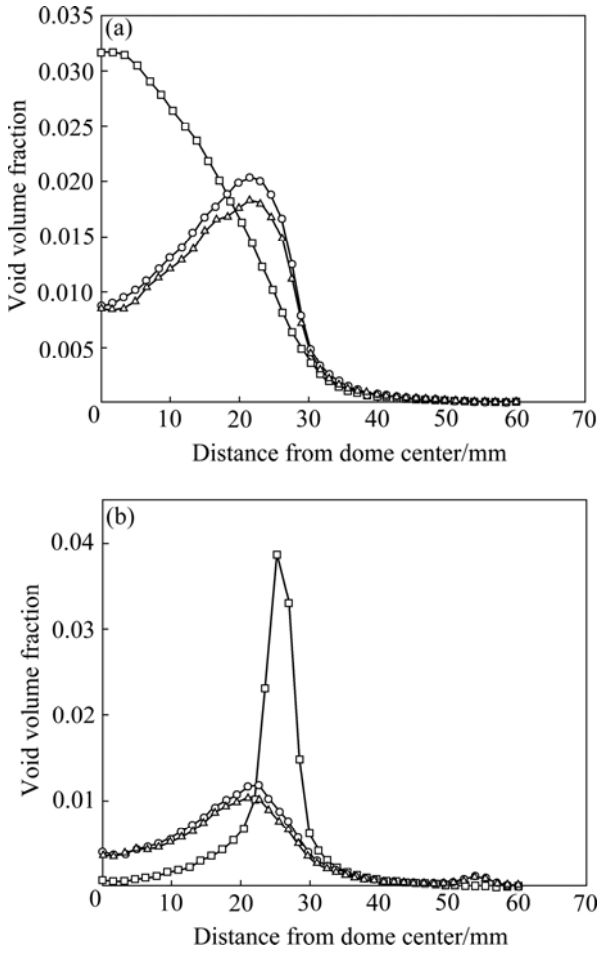

Fig. 5 Void volume fractions of outer skin sheet (a) and inner skin sheet (b)

4.3 Facture mode

Figure 6 shows the critical fracture location of three sandwich sheets. For Case 1, the critical fracture locates at inner skin sheet. But for other two cases, the critical fracture location occurs at outer skin sheet. It can be explained through analyzing the void volume fraction distribution for three cases in Section 4.2.

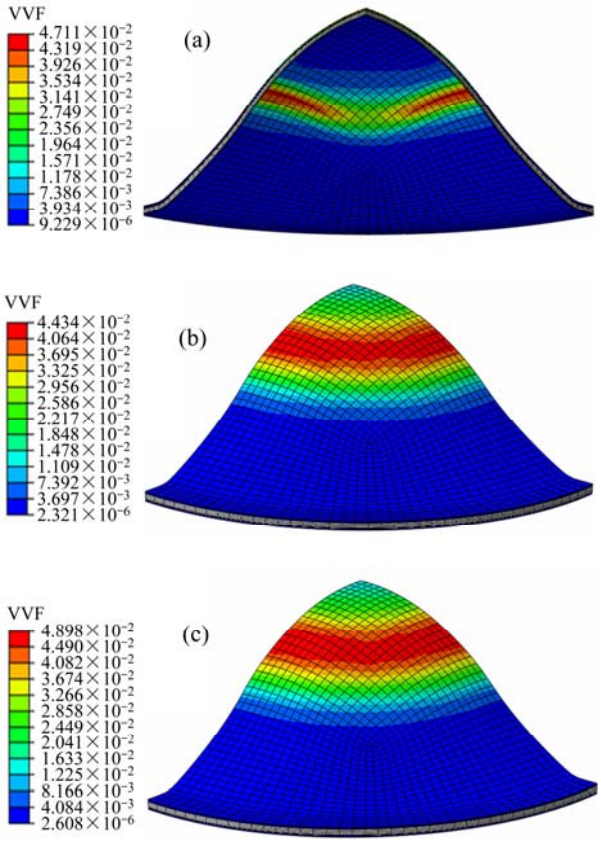

Fig. 6 Facture modes of three sandwich sheet for Case 1 (a), Case 2 (b) and Case 3 (c)

4.4 Forming limit diagram

Figure 7 shows the FLDs of three AA5052/ polyethylene/A5052 sandwich sheets. In Fig. 7, the predicted FLD diagram of sandwich under interfacial adhesion condition was compared with experimental one. The simulated FLD is a little higher than that of experimental measurement. The FLD of three-layer sheet is higher than that of monolithic sheet. It can be contributed to the friction effect of core polymer on improving the formability of skin sheet [13]. Figure 7 also shows the effect of interfacial adhesion strength on FLD of sandwich sheets. The FLD of sandwich sheet under stick interface condition is higher than that of other two conditions. It can be concluded that the FLD of sandwich sheet shift to higher value as the interfacial strength increase. So, the interface stress is beneficial to improving the FLD of sandwich sheet.

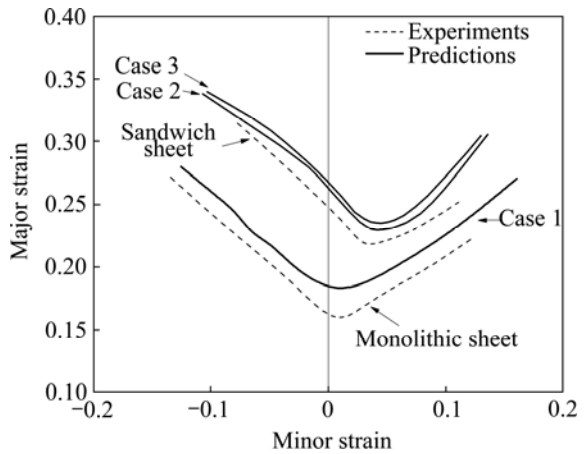

Fig. 7 FLD of sandwich sheets with different interfacial conditions

5 Conclusions

1) A GTN damage model based numerical simulation method considering the interface condition between skin sheet and core materials is successfully used to simulate the influence of adhesion strength on the formabilities of sandwich sheet.

2) The interface stress between skin sheet and core polymer can suppress the increase of void volume fraction of sandwich sheet and then postpone the fracture of skin sheet.

3) The sandwich sheet with the stick interfacial condition has the highest formability and the FLD of AA5052/polyethylene/AA5052 sandwich sheet shifts to higher value with increasing the interfacial adhesion strength.

References

[1] HAYASHI H, NAKAGAWA T. Recent trends in sheet metals and their formability in manufacturing automotive panels [J]. Journal of Materials Processing Technology, 1994, 46(3−4): 455−487.

[2] MILLER W K. Metal−plastic laminates for vehicle weight reduction [C]// SAE International Congress. Detroit: SAE, 1980: 1−10.

[3] DICELLO J A. Steel-polypropylene-steel laminate—A new weight reduction material [C]// SAE International Congress. Detroit: SAE, 1980: 1−15.

[4] YAO H, CHEN C C, LIU S D, LI K P, DU C, ZHANG L. Laminated steel forming modeling techniques and experimental verifications [C]// SAE International Congress. Detroit: SAE, 2003: 1−10.

[5] VEENSTRA E W. Aluminum-Plastic-Aluminum sandwich sheet for maximum weight reduction in body panels [C]//SAE International Congress. Detroit: SAE, 1993: 1−10.

[6] KEE J K, RHEE H M, CHOI B I, KIM C W, SUNG C W, HAN C P, KANG K W, WON S T. Development of application technique of aluminum sandwich sheets for automotive hood [J]. International Journal of Precision Engineering and Manufacturing, 2009, 10(4): 71−75.

[7] COMPSTON P, CANTWELL W J, CARDEW-HALL M J, KALYANASUNDARAM S, MOSSE L. Comparison of surface strain for stamp formed aluminum and an aluminum-polypropylene laminate [J]. Journal of Materials Science, 2004, 39(19): 6087−6088.

[8] PARSA M H, ETTEHAD M, MATIN P H, AHKAMI S N A. Experimental and numerical determination of limiting drawing ratio of Al3105-Polypropylene-Al3105 sandwich sheets [J]. Transaction of ASME Journal of Engineering Materials and Technology, 2010, 132(3): 1−11.

[9] MAKINOUCHI A, YOSHIDA S, OGAWA H. Finite element simulation of bending process of steel-plastic laminate sheets [J]. Journal of the JSTP, 1988, 29(330): 755−760.

[10] LIU J G, WANG Z J, MENG Q Y. Numerical investigations on the influence of superimposed double-sided pressure on the formability of biaxially stretched AA6111-T4 sheet metal [J]. Journal of Materials Engineering and Performance, 2012, 21(4): 429−436.
[11] UTHAISANGSUK V, PRAHL U, MUNSTERMANN S, BLECK W. Experimental and numerical failure criterion for formability prediction in sheet metal forming [J]. Computational Materials Science, 2008, 43(1): 43−50.
[12] TVERGAARD V, NEEDLEMAN A. Analysis of the cup-cone fracture in a round tensile bar [J]. Acta Metallurgica, 1984, 32(1): 157−169.
[13] NEEDLEMAN A, TVERGAARD V. An analysis of ductile rupture in notched bars [J]. Journal of the Mechanics and Physics of Solids, 1984, 32(6): 461−490.
[14] CHU C C, NEEDLEMAN A. Void nucleation effects in biaxially stretched sheets [J]. Transaction of ASME, Journal of Engineering Materials and Technology, 1980, 102(3): 249−256.
[15] LIU J G, XUE W. Experimental research on the formability of AA5052/Polyethylene/AA5052 sandwich sheets [J]. Transaction of Nonferrous Metals Society of China. (Accepted)
[16] LIU J G, LIU W, XUE W. Forming limit diagram prediction of AA5052/polyethylene/AA5052 sandwich sheets [J]. Materials and Design, 2013, 46(1): 112−120.

界面黏接强度对 AA5052/聚乙烯/AA5052 复合层板成形性影响

刘建光[1,2]，刘 伟[1,2]，王静宣[2]

1. 哈尔滨工业大学 金属精密热加工国家级重点实验室，哈尔滨 150001；
2. 哈尔滨工业大学 材料科学与工程学院，哈尔滨 150001

摘 要：研究 AA5052/聚乙烯/AA5052 复合层板成形过程中表层面板与中心聚合物层界面黏接强度对其成形性的影响规律。考虑复合层板界面特性，建立有限元分析模型模拟复合层板成形过程，通过对比实验与数值模拟计算，验证有限元模型的可靠性。分别对 3 种界面条件(分离，胶接和完全黏结)的复合层板进行刚性半球凸模实验和 NAKAZIMA 成形实验，研究复合层板界面黏接强度对表层铝板损伤行为及成形极限图的影响规律。研究结果表明：界面应力可以抑制孔洞体积分数的增加，延迟表层铝板断裂的发生。因此，完全黏结界面条件复合层板成形极限图最高，并且随着界面黏接强度的提高，复合层板成形极限图提高。

关键词：复合层板；成形性；界面黏接强度；铝；聚乙烯；数值方法；损伤模型

(Edited by DENG Lü-xiang)